Divalent Europium in $^1_\infty[Eu(Pz)_2(Pz\text{-}H)_2]$: The First Unsubstituted Pyrazolate and Cp Analogous Pyrazole Complex of a Rare Earth Element in One[#]

Catharina C. Quitmann and Klaus Müller-Buschbaum

Institut für Anorganische Chemie, Universität zu Köln, Greinstraße 6, D-50939 Köln, Germany

Reprint requests to Dr. Klaus Müller-Buschbaum. Fax: +49 (0)221 470 5083.
E-mail: Klaus.Mueller-Buschbaum@uni-koeln.de

Z. Naturforsch. **59b,** 562 – 566 (2004); received December 15, 2003

Bright yellow crystals of $^1_\infty[Eu(Pz)_2(Pz\text{-}H)_2]$ were obtained by the reaction of europium metal with a melt of pyrazole. According to single crystal X-ray analysis the compound exhibits a one-dimensional chain structure including both unsubstituted pyrazolate anions as well as unsubstituted neutral pyrazole molecules as ligands. The latter are isoelectronic with the cyclopentadienyl anion and link two adjacent Europium(II) centers in an η^1-σ-bridging as well as Cp analogous η^5-π-binding mode, whilst the pyrazolate anions are N-η^1-coordinating terminal ligands. In addition to the crystal structure, MIR, FarIR, Raman and UV/vis spectroscopic data are presented.

Key words: Lanthanides, Pyrazole, Crystal Structure, Europium

Introduction

Aside from cyclopentadienyl (Cp) and complexes with oxygen donor atoms [1-3], amides form another pillar of the coordination chemistry of the rare earth elements [4]. The oxophilic character of the rare earth elements complicates both the synthesis of complete nitrogen coordination spheres as well as the formation of homoleptic complexes of the rare earth elements with nitrogen donors [5]. The main reason can be found in omnipresent coordinating solvent molecules used in the classic solvent synthesis routes. It can be shown, however, that solid state chemistry approaches towards this chemistry including melt and solvothermal syntheses in the absence of any solvent offer a useful route towards homoleptic amides of the rare earth elements [6], especially if the crystallisation of the products can be accomplished under reaction conditions [7 – 10] according to eq. (1):

$$Ln + x(R_2\text{-}NH) \longrightarrow Ln(N\text{-}R_2)_x + \frac{x}{2}H_2 \qquad (1)$$

Without decomposition of the ligand, the rare earth elements are oxidised by the amines releasing hydrogen. These solvent free methods of synthesis furthermore offer the possibility to react even the smallest stable N-heterocycles such as pyrrole and pyrazole (Pz-H). And though substituted pyrazoles, mainly bis-^{t}Butyl-pyrazoles [11, 12] or borato-pyrazoles [13, 14], have been successfully employed in obtaining homoleptic amides, neither unsubstituted pyrazolates nor unsubstituted pyrazole-N-donor complexes of the rare earth elements can be found in the literature. Here we present $^1_\infty[Eu(Pz)_2(Pz\text{-}H)_2]$, the first unsubstituted pyrazolate and the first unsubstituted Cp analogous pyrazole complex of the rare earth elements.

Results and Discussion

Synthesis

Due to the high reactivity of the rare earth elements, the title compound can be synthesised from europium metal and excess pyrazole in a solvent-free melt reaction in evacuated sealed glass ampoules at 185 °C according to eq. (2). Except for the excess of pyrazole the reaction gives a single product. To enhance the reactivity europium was dissolved in liquid ammonia prior to the reaction. Evaporation of the ammonia gave finely dispersed metal.

$$Eu + 4Pz\text{-}H \longrightarrow {}^1_\infty[Eu(Pz)_2(Pz\text{-}H)_2] + H_2 \qquad (2)$$

[#] Pz-H = Pyrazole, C_3H_3NNH; Pz = Pyrazolate, $C_3H_3N_2^-$; Cp = Cyclopentadienyl anion, $C_5H_5^-$

0932–0776 / 04 / 0500–0562 $ 06.00

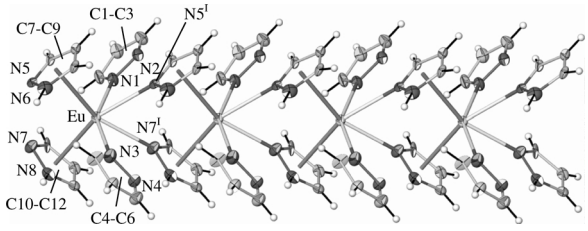

Fig 1. The polymeric chain structure of $^1_\infty$[Eu(Pz)$_2$(Pz-H)$_2$]. The thermal ellipsoids represent 50% of the probability levels. Pz-H molecules coordinate Eu η^5 and η^1 linking the building units whilst pyrazolate ligands only show η^1-coordination. Symmetry operation: I: $x+1, y, z$.

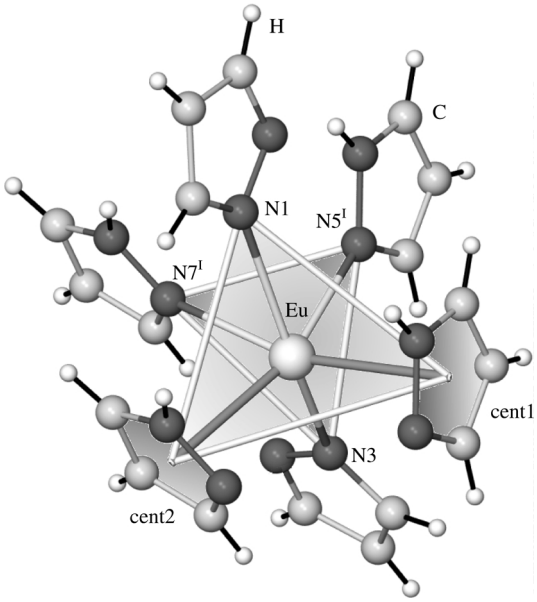

Fig 2. The trigonal antiprismatic coordination sphere of Eu^{II} in $^1_\infty$[Eu(Pz)$_2$(Pz-H)$_2$]. Each Eu is surrounded by four Pz-H and two Pz ligands giving Eu(Pz)$_2$(Pz-H)$_{4/2}$. η^5-π-interactions to Pz-H molecules are depicted by shaded pyrazole rings. Eu is drawn as a large light ball, N atoms as smaller dark balls, C atoms as smaller light balls and H atoms as small white balls. Symmetry operation: I: $x+1, y, z$, cent1: N5, N6, C7-9, cent2: N7, N8, C10-12.

Crystal structure

$^1_\infty$[Eu(Pz)$_2$(Pz-H)$_2$] (Pz-H = pyrazole, C_3H_3NNH; Pz = pyrazolate anion, $C_3H_3N_2^-$) exhibits a one-dimensional chain structure of Eu(Pz)$_2$(Pz-H)$_{4/2}$ units (see Fig. 1). The coordination sphere of Eu can be described as a trigonal antiprism of a big triangle of one N atom of a Pz-H molecule and two η^5-coordinating Pz-H rings as well as a smaller triangle of three N atoms belonging to two Pz anions and one

Table 1. Crystallographic data for $^1_\infty$[Eu(Pz)$_2$(Pz-H)$_2$]. Deviations are given in brackets.

Formula	$C_{12}H_{14}N_8Eu$
Cell constants, (a,b,c)(pm)	$a = 471.0(2)$;
	$b = 797.8(4)$;
	$c = 992.1(5)$;
$(\alpha,\beta,\gamma)(^\circ)$	$\alpha = 97.23(4)$;
	$\beta = 103.79(4)$;
	$\gamma = 90.21(4)$
V (10^6 pm^3)	359.0(3)
Z	1
T (K)	170
$d_{calcd.}$ (g·cm^{-3})	1.953
X-ray radiation	Mo-K$_\alpha$, $\lambda = 71.07$ pm
Diffractometer	STOE IPDS II
Crystal system, space group	triclinic, $P\bar{1}$
Flack parameter [27]	0.05(10)
Data range	$5.14 \le 2\theta \le 54.30$,
	$\Delta\theta = 2^\circ$, $\varphi = 0/90^\circ$
	$-6 \le h \le 5$;
	$-10 \le k \le 9$;
	$-12 \le l \le 12$
No. of measured reflections (all)	4858
No. unique reflections; R_{int} (all)	2733; 0.083
No. of parameters	190
Ratio reflections / parameters	14
Absorption coefficient μ (cm^{-1})	43.7
R_1[a] for n reflections with $F_o > 4\sigma(F_o)$; n	$R_1 = 0.042$; 2732
for all reflections	$R_1 = 0.042$
wR_2[b] (all)	$wR_2 = 0.106$
Remaining elec. density	$+1.3/-1.9$ e/pm·10^6

[a] $R_1 = \Sigma[|F_o| - |F_c|]/\Sigma[|F_o|]$; [b] $wR_2 = (\Sigma w(F_o^2 - F_c^2)^2/\Sigma w(F_o^4))^{1/2}$ [26].

N atom of a Pz-H ring (see Fig. 2). Counting each Pz-H ring in its Cp analogous binding mode as a six electron donor system, Eu has a coordination number of ten. The pyrazolate ligands each show only one σ-bond with the electron pair in the sp^2 hybrid orbital. Contrary to this the bulk of the known ^{t}Bu-pyrazolates exhibit η^2-binding of both neighbouring N atoms on the metal centres, independent of the oxidation state of the rare earth element [6, 11, 12, 15]. Only the small Er^{III} in [Er(^{t}Bu$_2$Pz)$_3$] shows an η^1-binding mode for a pyrazolate ligand [11]. The Cp analogous binding mode of the neutral pyrazole molecules in $^1_\infty$[Eu(Pz)$_2$(Pz-H)$_2$] has not yet been observed for rare earth compounds. It thus resembles the Cp complex [Cp$_2$Yb(Me$_2$Pz)$_2$] [16], though the Cp rings in this compound cannot connect the monomeric units to chains because of the lack of linking nitrogen atoms in Cp rings. The Eu-N distances in $^1_\infty$[Eu(Pz)$_2$(Pz-H)$_2$] range from 265 pm for Pz amides to 273–310 pm for pyrazole-N donor bonds and N atoms participating in the η^5-coordination, respectively, corresponding to

Table 2. Selected distances (pm) and angles (°) between atoms of $^1_\infty$[Eu(Pz)$_2$(Pz-H)$_2$]. Deviations are given in brackets.

Distances				*Angles*	
Eu-N7^{I}	265(2)	Eu-cent2	276	N1-Eu-N5^{I}	80.9(6)
Eu-N1	269.0(9)	Eu-C9	284.4(9)	N1-Eu-N7	98.8(6)
Eu-N3	272.8(9)	Eu-C10	296(1)	N3-Eu-N8	77.8(3)
Eu-N5^{I}	277(2)	Eu-C11	297.6(8)	N3-Eu-N5	77.8(6)
Eu-N8	287.5(8)	Eu-C12	307.3(9)	N6-Eu-N8	86.6(3)
Eu-N7	291(2)	N1-N2	132(1)	N6-Eu-N7	79.5(5)
Eu-N5	296(1)	N3-N4	133(2)	cent1-Eu-cent2	110.2
Eu-N6	310(1)	N5-N6	132(3)	cent1-Eu-N7^{I}	159.3
Eu-cent1	275	N7-N8	134(2)	cent2-Eu-N5^{I}	160.9

^{I}: Symmetry operation: $x+1, y, z$; cent1: N5, N6, C7-9; cent2: N7, N8, C10-12.

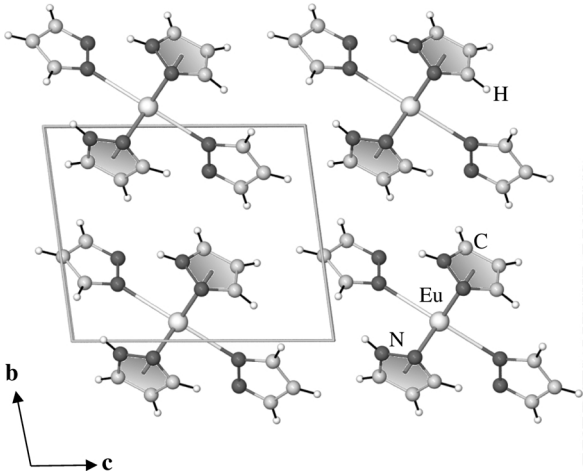

Fig 3. The crystal structure of $^1_\infty$[Eu(Pz)$_2$(Pz-H)$_2$].The view along [100] suits the chain direction. All chains run into the same direction giving an acentric structure with a small triclinic unit cell. Eu atoms are drawn as large light balls, N atoms as smaller dark balls, C atoms as smaller light balls and H atoms as small white balls.

other divalent Eu-N complexes like $^1_\infty$[Eu(C$_{12}$H$_8$N)$_2$] with Eu^{II}-N in the range of 253 – 268 pm [9]. For Eu^{III}-N the distances had to be significantly shorter like in the homoleptic pyridylbenzimidazolate [Ln(N$_3$C$_{12}$H$_8$)$_2$(N$_3$C$_{12}$H$_9$)$_2$][Ln(N$_3$C$_{12}$H$_8$)$_4$](N$_3$C$_{12}$H$_9$)$_2$ [8] with 244 – 246 pm for Eu^{III}-N amide distances and 259 – 267 pm for Eu^{III}-N amine distances. The Eu-η^5-(Pz-H) distances of the π-interaction also match with the divalent state of Eu in the homoleptic carbazolate $^1_\infty$[Eu(C$_{12}$H$_8$N)$_2$] and its η^6-π-interactions with an average of 301 pm [9] (see Table 2 for selected atom distances of $^1_\infty$[Eu(Pz)$_2$(Pz-H)$_2$]). Therefore Pz and Pz-H ligands can be clearly distinguished in the title compound. As all strands run into the same direction, the structure of $^1_\infty$[Eu(Pz)$_2$(Pz-H)$_2$] is acentric (see Fig. 3). The borato pyrazolates of the rare earth elements are not suitable for comparison as one of their nitrogen atoms is engaged in the N-B bonds [13, 14, 17] and therefore cannot participate in Ln-N coordination.

Spectroscopic investigations

In order to confirm the results of the single crystal X-ray diffraction analysis $^1_\infty$[Eu(Pz)$_2$(Pz-H)$_2$] was also investigated by MIR, FarIR, Raman and UV/vis spectroscopy. The FarIR and Raman spectra show the significant Eu-N stretching modes (FarIR: 220, 196, 168 cm^{-1}; Raman: 196, 165, 135 cm^{-1}), and which cannot be observed in the ligand spectra. Whilst the FarIR bands of the title compound show distinct shifts due to the different coordination modes, the Raman bands exhibit only a slight shift in comparison to Eu^{II}-N vibrations in $^1_\infty$[Eu(C$_{12}$H$_8$N)$_2$] (FarIR: 170, 157, 109 cm^{-1}; Raman: 203, 178, 152 cm^{-1}) [9] and are thereby in the region of known Ln-N vibrations [7, 8, 10, 11, 19]. In comparison to the vibration bands of the free ligand several bands in the MIR and Raman spectra show identical positions (IR: 3122, 2979, 2859, 1398, 1359, 1313, 1150, 936, 922, 884, 758, 615, 74 cm^{-1}) whereas others show a hypsochromic shift (IR: 2928, 1567, 1524, 1481, 1266, 1202, 1052, 1038, 855, 681, 118, 100 cm^{-1}) reflecting the coordination of both pyrazole and pyrazolate ligands to the Eu centers. The region of 1100 – 1400 cm^{-1} shows a variety of bands known for aromatic N-heterocycles [20]. The band pattern above 3100 cm^{-1} can be assigned to N-H and C-H stretch modes [21]. It is almost identical to Pz-H and confirms that $^1_\infty$[Eu(Pz)$_2$(Pz-H)$_2$] contains unreacted pyrazole molecules.

Further evidence for the divalent state of Eu is given by electron absorption spectroscopy. The absorption spectrum of $^1_\infty$[Eu(Pz)$_2$(Pz-H)$_2$] shows none of the characteristic *f-f* transitions of trivalent Eu but a region without bands resembling the Diecke diagram of Gd^{III} and thus Eu^{II} [22]. The absorption band between 300 and 400 nm can be identified as *f-d* transitions of Eu^{II} [23] as well as ligand–metal charge transfer processes. However, it overlaps with the absorption of the ligands around 400 nm and thus can only be assigned by comparison of the ligand and product spectra. The product spectrum shows a shift to red compared to the ligand pyrazole due to ligand metal interactions responsible for the yellow to orange colour of the compound. For comparison, both the free pyrazole ligand as well as the Eu^{III} compound

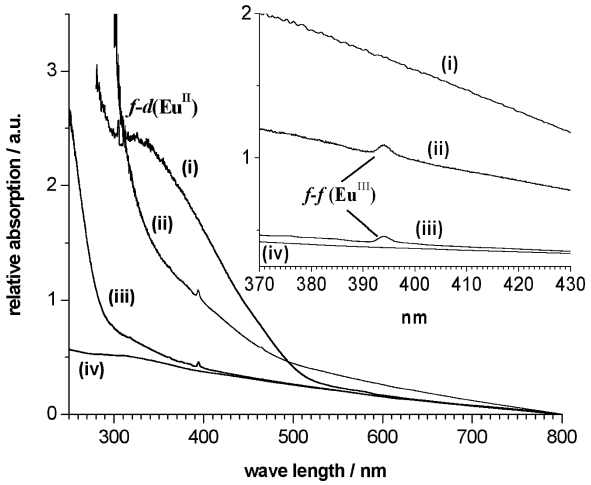

Fig 4. The UV/vis spectra of $^1_\infty$[Eu(Pz)$_2$(Pz-H)$_2$] (i), its oxidation and decomposition product in EtOH (ii), $(NH_4)_3EuCl_6$ (iii) and pyrazole (iv) in the range of 250–800 nm. The inserted graphic shows a *f-f* transition for Eu^{III}, which cannot be observed for $^1_\infty$[Eu(Pz)$_2$(Pz-H)$_2$].

$(NH_4)_3EuCl_6$ were investigated regarding their absorption properties. Moreover, $^1_\infty$[Eu(Pz)$_2$(Pz-H)$_2$] was further oxidised with EtOH and an absorption spectrum of the product collected. Both $(NH_4)_3EuCl_6$ and the decomposition product in EtOH show a *f-f* transition at 395 nm, characteristic for Eu^{III}, which cannot be observed for $^1_\infty$[Eu(Pz)$_2$(Pz-H)$_2$] and Eu^{II} in general (see Fig. 4).

Conclusions

The solid state chemistry reaction route of the high temperature oxidation of rare earth elements with amines proved a suitable pathway for obtaining $^1_\infty$[Eu(Pz)$_2$(Pz-H)$_2$] and therefore both the first unsubstituted pyrazolate as well as unsubstituted Cp analogous pyrazole complex of the rare earth elements in one. In the absence of any solvent no competition with solvent molecules can occur, a necessary requirement for the formation of compounds like $^1_\infty$[Eu(Pz)$_2$(Pz-H)$_2$]. In order to saturate the coordination sphere around the large Eu^{II} ions [18], unreacted pyrazole from the melt is acquired instead. Whilst the melt reaction can be successfully used to react and crystallise products from unsubstituted pyrazole, previous solvent approaches made a substitution of the Pz ligand necessary to allow a certain solubility in solvents both for recrystallisation and reaction [6, 11, 12, 15]. Unsubstituted $^1_\infty$[Eu(Pz)$_2$(Pz-H)$_2$] shows a new binding mode of the rare earth elements, especially of pyrazole as an η^5-coordinating ring system, the free electron pair in a sp^2-N orbital furthermore linking the building units to chains. This is in good accordance with the 1-N ligand carbazole ($C_{12}H_8NH$), which also saturates the coordination spheres of Yb, Eu and Sm with additional π-interactions and hence also forms one-dimensional structures [9, 24]. In combination with the results of single crystal X-ray diffraction analysis electron absorption spectroscopy proves the divalent character of europium.

Experimental Section

Eu metal was treated with hexane to cleanse it of packing oil (ChemPur). Pyrazole (ACROS) was used as delivered. Because of the air and moisture sensitivity of both Eu and the product all treatments were carried out using standard Schlenk, glove box and vacuum line techniques. The Eu metal was dissolved in liquid ammonia prior to the reaction. Evaporation of ammonia gave finely dispersed metal. The IR spectra were recorded using a BRUKER FTIR-IS66V-S spectrometer, the Raman spectra using a BRUKER FRA 106-S spectrometer. The absorption spectroscopy was carried out on a VARIAN Carey 05E spectrometer.

$^1_\infty$[Eu(Pz)$_2$(Pz-H)$_2$]

Eu (1 mmol = 152 mg) und pyrazole (C_3H_3NNH, Pz-H, 6 mmol = 408 mg) were sealed in an evacuated glass ampoule and heated in 13 h to 185 °C. The reaction temperature was held for two weeks. The reaction mixture was then cooled down to 50 °C in 395 h and to room temperature in 10 h. The reaction product was a yellow to orange crystalline material containing no unreacted europium metal. In order to obtain the pure product the excess Pz-H was sublimed to the other side of the ampoule in a temperature gradient from 80 °C to room temperature in 3 h to give transparent yellow to orange crystals of $^1_\infty$[Eu(Pz)$_2$(Pz-H)$_2$].

UV/vis: λ_{max} = 250, 330 nm. – MIR (KBr): $\tilde{\nu}$ = 3148, 3122, 2979, 2928, 2859, 1567, 1524, 1481, 1438, 1398, 1359, 1313, 1266, 1239, 1223, 1202, 1151, 1131, 1052, 1038, 936, 922, 884, 872, 855, 758, 681, 628, 615 cm^{-1}. – FarIR (PE): $\tilde{\nu}$ = 584, 359, 220, 195, 168, 130, 118, 100, 74 cm^{-1}. – Raman: $\tilde{\nu}$ = 3143, 3121, 3093, 1480, 1469, 1401, 1358, 1264, 1222, 1141, 1125, 1051, 1023, 1015, 918, 902, 196, 165, 135, 110, 74 cm^{-1}. – $C_{12}H_{14}N_8Eu$ (422.27): calcd. C 34.2, H 3.3, N 26.5; found C 33.8, H 3.5, N 26.2.

Pyrazole

UV/vis: λ_{max} = 250 nm. – MIR (KBr): $\tilde{\nu}$ = 3155, 3124, 3052, 2974, 2919, 2858, 2809, 1642, 1558, 1514, 1468, 1397, 1358, 1310, 1257, 1150, 1137, 1056, 1033, 937, 920,

883, 878, 839, 758, 653, 618 cm^{-1}. – FarIR (PE): $\tilde{\nu} = 420$, 353, 136, 123, 110, 106, 94, 72 cm^{-1}.

Prior to the data collection five crystals of $^1_\infty$[Eu(Pz)$_2$(Pz-H)$_2$] were investigated concerning their quality on a STOE IPDS-II diffractometer. A crystal of $(0.3 \times 0.3 \times 0.2)$ mm^3 was selected for single crystal X-ray diffraction analysis and the data collection was carried out at 170 K. The structure model was obtained with direct methods [25] and all non-hydrogen atoms were refined anisotropically by the least square method [26]. $^1_\infty$[Eu(Pz)$_2$(Pz-H)$_2$] crystallises in the triclinic crystal system in the space group $P\bar{1}$. Table 1 contains the crystallographic data, Table 2 selected interatomic distances and angles between atoms of $^1_\infty$[Eu(Pz)$_2$(Pz-H)$_2$]. Further information about the single crystal X-ray analysis was deposited at the Cambridge Crystallographic Data Centre, CCDC, 12 Union Road, Cambridge CB2 1EZ, UK (fax: +44 1223336033 or e-mail: deposit@ccdc.cam.ac.uk) and may be requested by citing the deposition number CCDC-228083, the names of the authors and the literature citation.

Acknowledgements

We thank the Fonds der Chemischen Industrie for supporting this work with a "FCI-PhD" scholarship, PD Dr. Angela Möller for electron absorption spectroscopy measurements, and Prof. Dr. Gerd Meyer for his generous financial support and equipment.

[1] H. Schumann, Angew. Chem. **96**, 475 (1984); Angew. Chem. Int. Ed. **23**, 474 (1984).
[2] S. Arndt, J. Okuda, Chem. Rev. **102**, 1953 (2002).
[3] H. Schumann, J. A. Meese-Marktscheffel, L. Esser, Chem. Rev. **95**, 865 (1995).
[4] R. Kempe, Angew. Chem. **112**, 478 (2000); Angew. Chem. Int. Ed. **39**, 468 (2000).
[5] P. J. Davidson, M. F. Lappert, R. Pearce, Acc. Chem. Res. **7**, 209 (1974).
[6] G. B. Deacon, A. Gitlits, P. W. Roesky, M. R. Bürgstein, K. C. Lim, B. W. Skelton, A. H. White, Chem. Eur. J. **7**, 127 (2001).
[7] K. Müller-Buschbaum, Z. Anorg. Allg. Chem. **628**, 2731 (2002).
[8] K. Müller-Buschbaum, C. C. Quitmann, Inorg. Chem. **42**, 2742 (2003).
[9] K. Müller-Buschbaum, C. C. Quitmann, Z. Anorg. Allg. Chem. **629**, 1610 (2003).
[10] K. Müller-Buschbaum, Z. Anorg. Allg. Chem. **629**, 2127 (2003).
[11] D. Pfeiffer, B. J. Ximba, L. M. Liable-Sands, A. L. Rheingold, M. J. Heeg, D. M. Coleman, H. B. Schlegel, T. F. Kuech, C. H. Winter, Inorg. Chem. **38**, 4539 (1999).
[12] G. B. Deacon, C. M. Forsyth, S. Nickel, S. J. Organomet. Chem. **647**, 50 (2002).
[13] M. V. R. Stainer, J. Takats, Inorg. Chem. **21**, 4050 (1982).
[14] C. Apostolidis, J. Rebizant, B. Kanellakopolos, R. von Ammon, H. Dornberger, J. Muller, B. Powietzka, B. Nuber, Polyhedron **16**, 1057 (1997).
[15] G. B. Deacon, A. Gitlits, B. W. Skelton, A. H. White, J. Chem Soc., Chem. Commun. 1213 (1999).
[16] X. Zhou, Z. Huang, R. Cai, L. Zhang, L. Zhang, X. Huang, Organometallics **18**, 4128 (1999).
[17] C. Apostolidis, J. Rebizant, O. Walter, B. Kanellakopolos, H. Reddmann, H.-D. Amberger, Z. Anorg. Allg. Chem. **628**, 2013 (2002).
[18] R. D. Shannon, Acta Crystallogr. **A32**, 751 (1976).
[19] M. S. Haghighi, C. L. Teske, H. Homborg, Z. Anorg. Allg. Chem. **608**, 73 (1992).
[20] B. Schrader, Raman/ Infrared Atlas of Organic Compounds, 2nd Edition, Wiley VCH, Weinheim (1989).
[21] J. Weidlein, U. Müller, K. Dehnicke, Schwingungsfrequenzen II, Nebengruppenelemente, Georg Thieme Verlag, Stuttgart (1986).
[22] G. Blasse, B. C. Grabmeier, Luminescent Materials, p. 26, Springer, Berlin (1984).
[23] P. Dorenbos, J. Phys. Condens Mat. **15**, 575 (2003).
[24] K. Müller-Buschbaum, C. C. Quitmann, Z. Kristallogr. Suppl. **19**, 47 (2002).
[25] G. M. Sheldrick, SHELXS-86, Programm zur Lösung von Kristallstrukturen, Göttingen (1986).
[26] G. M. Sheldrick, SHELXL-97, Programm zur Verfeinerung von Kristallstrukturen, Göttingen (1997).
[27] H. D. Flack, Acta Crystallogr. **A39**, 876 (1983).